

## Optical properties in conjugated polymers

This article has been downloaded from IOPscience. Please scroll down to see the full text article.

2008 J. Phys.: Condens. Matter 20 064231

(<http://iopscience.iop.org/0953-8984/20/6/064231>)

View [the table of contents for this issue](#), or go to the [journal homepage](#) for more

Download details:

IP Address: 129.252.86.83

The article was downloaded on 29/05/2010 at 10:32

Please note that [terms and conditions apply](#).

# Optical properties in conjugated polymers

Y Zempo, N Akino, M Ishida, M Ishitobi and Y Kurita

Sumitomo Chemical Co., Ltd, 6 Kitahara, Tsukuba 300-3294, Japan

E-mail: [zempo@tuc.sumitomo-chem.co.jp](mailto:zempo@tuc.sumitomo-chem.co.jp)

Received 3 September 2007, in final form 14 November 2007

Published 24 January 2008

Online at [stacks.iop.org/JPhysCM/20/064231](http://stacks.iop.org/JPhysCM/20/064231)

## Abstract

Optical properties in conjugated polymers such as poly(*p*-phenylenevinylene) and poly(9,9-dialkyl-fluorene) have been studied using time-dependent density functional theory. In the calculations of the optical properties, real-space and real-time techniques are employed. We follow the linear responses of the systems under externally applied perturbations in the real time. To estimate the polymer spectra, we have calculated the responses of oligomers of different lengths and obtained the extrapolated values. The estimated polymer spectra agree with the experiments reasonably well.

(Some figures in this article are in colour only in the electronic version)

## 1. Introduction

Polymer light emitting diodes (PLEDs) are of interest for thin flat panel displays and other lighting applications [1]. One of the advantages of PLEDs is the simplicity of the device structure, consisting of the light emitting layer of conjugated polymers between a cathode and an anode. The emission color is basically determined by the nature of polymer, thus the color tuning and efficiency are considered to be controlled by the manipulation of the molecular structures. On the other hand, the device optimization requires us to understand the fundamental physics of the charge injection, transport, and recombination. Thus, intensive investigations of both the material design and the device optimization are expected to achieve better performance in PLEDs.

As candidate materials in PLEDs, for example, polyacetylene, poly(*p*-phenylene), poly(*p*-phenylenevinylene) (PPV), polythiophene, poly(9,9-dialkyl-fluorene) (PFL) and their substituted derivatives are expected to be basic materials, and their electronic structures have been extensively studied [6] since the discovery of metallic-like electrical conductive properties by Heeger, MacDiarmid, Shirakawa, and co-workers in 1977 [2, 3].

We have focused on the optical spectra of the conjugated polymers as one of the most important properties in real applications. In the practical polymers, various substituents and copolymerization are frequently used as molecular design techniques to control optical properties. For examples, amines could be incorporated into the main chain as emission centers. These possibilities in polymers are one of the advantages in the real applications, but make computational modeling more

difficult. In addition to the diversity, the polymer structures are generally amorphous-like and are usually difficult to handle as periodic systems. For the latter, there are several successful applications to homo-polymers to describe conjugate polymers in a crystal cell in dependence on oligomer length [4, 5]. Although, depending on the polymer structures, one could use periodic systems, we have adopted a single chain system in free boundary conditions for simplicity.

Besides taking into account the excitonic effects, the dielectric tensor has been calculated by solving the Bethe–Salpeter equation for the electron–hole Green’s function [6]. These effects are not involved in our calculation, because the purpose of this paper is to estimate the spectrum using a single chain model, and of particular interest to us is not the precise calculation of the spectrum, but the estimation of the spectrum shape of the polymer from the calculations of small sizes of oligomers.

Relating to thermal motions, Poolmee *et al* [7] have reported that the effect of the dihedral angle on the excited state was examined and the accurate absorption spectra were simulated by taking the thermal average for the conformers of the dihedral angle. We have utilized this technique and applied it to the effect of the dihedral angle between amine and connecting FL to obtain the optical spectrum.

The time-dependent density functional theory (TDDFT) has become one of the most prominent and most widely used for the calculation of excited states of medium-sized to large molecules, and recognized as a powerful tool for opto-electronic behaviors [8, 9]. TDDFT is in principle capable of treating these sorts of behaviors, if the exact local exchange–correlation (xc) functional is known. An approximate xc

functional has to be chosen in any practical calculation. Although the functional has been developed with respect to the electronic ground state, it yields accurate results for valence–excited states in the case where the excitation energy is well below the ionization potential [9]. Within this framework, in which the interaction of the electron and the hole are at the LDA level, we have applied TDDFT to study of the optical properties of our conjugated polymers.

In this paper, we present the results of our TDDFT simulations for the oligo-PV and oligo-FL, as typical examples of conjugated polymers, PPV and PFL, respectively. In the next section, we describe the theory with our numerical details. The results of its applications follow, and we summarize our results and conclusions in the last section.

## 2. Theory and numerical details

In this section, we briefly present our TDDFT calculation procedure. One of the most successful ways of obtaining the electronic structure from first principles is the use of computational approaches based on the density functional theory (DFT) [10] with the local density approximation (LDA). The total energy of the ground state can be derived from the Kohn–Sham equation (KS) [11]. Although, for the excited states, it is much less successful in describing the optical responses and the excitation spectra, this difficulty is, in principle, solved by the extension of DFT to the time-dependent theory. Its foundation was established by Runge and Gross [8]. In analogy to the time-independent case, the TDDFT equation of motion coupled with pseudopotentials is given by

$$\left\{-\frac{1}{2}\nabla^2 + V_{\text{ion}}^{\text{ps}}(\mathbf{r}) + V_{\text{H}}(\mathbf{r}, t) + V_{\text{XC}}[\rho(\mathbf{r}, t)] + V_{\text{ext}}(\mathbf{r}, t)\right\} \times \psi_i(\mathbf{r}, t) = i\frac{\partial}{\partial t}\psi_i(\mathbf{r}, t), \quad (1)$$

where  $V_{\text{ion}}^{\text{ps}}$  is an ionic pseudopotential,  $V_{\text{H}}$  is the Hartree potential, and  $V_{\text{XC}}$  is the exchange–correlation potential. Since the exact time-dependent xc kernel is not known, the originally non-local time-dependent xc kernel is replaced with a time-independent local one. This is considered as reasonable when the density varies slowly with time. This approximation allows the use of a standard local ground state xc functional in the TDDFT framework. The Hartree and exchange–correlation potentials can be determined from the electronic charge density,  $\rho(\mathbf{r}, t) = \sum_i |\psi_i(\mathbf{r}, t)|^2$ . The summation is over all occupied states  $i$ . The Hartree potential is determined by  $\nabla^2 V_{\text{H}} = -4\pi\rho$ , and as the xc potential,  $V_{\text{XC}}$ , the usual local density approximation (LDA) is used in our study. For the ionic potential, we employ the pseudopotential  $V_{\text{ion}}^{\text{ps}}$  in the separable form so that only the valence electrons are considered [12]. Prior to the calculation of optical responses, we first solve the usual, time-independent formulation of the pseudopotential-DFT method [13] to obtain the optimized electronic structure [14]. Then, we apply an external field  $V_{\text{ext}}$  to the system as a perturbation and follow the linear responses of the system in real time.

This method is effectively used for the cases where the potential is time dependent, e.g. the time-dependent behaviors

of electrons in oscillating electric and magnetic fields, and excited state reactions [15]. Empirically, we know that these can be described fairly well by TDDFT. Although the xc functional that we adopted has been developed with respect to the electronic ground states, we have also employed it in our practical calculations.

In our calculations, the real-time and real-space technique is adopted in solving equation (1) by the finite difference approach [16] without using explicit bases such as plane waves [17] and Gaussians [18]. Within the framework of this approach, we can solve for the wavefunctions on the grid with a fixed domain, which encompasses the physical system of interest. A uniform grid is used in our study for simplicity.

The wavefunctions are evolved by the time evolution operator,  $\psi(t) = \exp[-iHt]\psi(0)$ , with the initial wavefunction at  $t = 0$ ,

$$\psi_i|_{t=0} = e^{ik_z z}\psi_i(0), \quad (2)$$

where  $H$  is the Hamiltonian of the system, and  $k_z$  is a small wavenumber corresponding to the external perturbation in the  $z$  direction. In the linear response, the time-dependent polarizability is proportional to the dipole matrix element  $\mu_{z_i}(t) = \langle \psi(t)|z_i|\psi(t) \rangle$ , where  $z_i$  with  $i = 1, 2$ , and  $3$  represents  $x$ ,  $y$ , and  $z$ , respectively. The frequency-dependent polarizability in the  $z$  direction  $\alpha_z(\omega)$  is then obtained as the time–frequency Fourier transformation of  $\mu_z(t)$ ,

$$\alpha_z(\omega) = \frac{1}{k} \int dt e^{-i\omega t} \mu_z(t). \quad (3)$$

The polarizability  $\alpha(\omega)$  is given by the orientation average,  $\alpha = (\alpha_x + \alpha_y + \alpha_z)/3$ . The optical strength function,  $S(\omega)$ , is related to the imaginary part of the polarizability,

$$S(\omega) = \frac{2\omega}{\pi} \text{Im} \alpha(\omega). \quad (4)$$

Since uniform spatial grids are used in our calculations to represent the electron wavefunctions, the grid spacing  $\Delta x$  and the total number of grid points  $N_x$  become important parameters. The grid spacing  $\Delta x$  is determined so that the Kohn–Sham eigenvalues converge within the order of  $O(10^{-1} \text{ eV})$ . This accuracy can be achieved with  $\Delta x = 0.3 \text{ \AA}$  in the hydrocarbon systems. The volume  $N_x(\Delta x)^3$  is determined by setting the distance between the edge and any atoms to be more than a certain value, which allows us to neglect the effect of the edge. One may use the absorption boundary condition to eliminate the reflection from the boundary.

For the time evolution, the time step  $\Delta t$  and the total number of time steps  $T$  have to be considered as additional important parameters. The time step  $\Delta t$  has to be short enough so that the single-particle Hamiltonian can be treated as being static. One may expect the dependence  $\Delta t \sim (\Delta x)^2$ . For the time evolution of wavefunctions, we have used the Taylor expansion of the time evolution operator up to fourth order [14]. The total length of time evolution  $T$  is related to the effective energy resolution in any physical quantity in interest such as the strength function. In our preliminary study

of the molecule  $C_{60}$ ,  $\Delta t = 0.001 \text{ eV}^{-1}$  is required for carbon structures with a grid size of  $\Delta x = 0.3 \text{ \AA}$ , and  $T = 10 \text{ eV}^{-1}$  gives the energy resolution of  $1/T = O(10^{-1} \text{ eV})$ . In this case, we can find the low energy absorption peaks at 3.5, 4.4, and 5.6 eV, which agree well with the experimentally observed peaks at 3.8, 4.8, and 5.8 eV [19].

One of the advantages of this real-space and real-time approach is that we can keep our program simple and understand physical meanings as directly as possible. The other is that the CPU time scales with the number of particles  $N$  and the spatial dimension  $D$  as  $O(ND) \sim O(N^2)$ , which becomes an advantage especially when we need to handle a large system. The time evolution is performed in real time, thus the total number of time steps is closely connected to the accuracy. To realize it, enough computational resources are required. However, it could be matched by recent progress in computers.

### 3. Absorption and fluorescence spectra

We investigate the dependence of the oligomer length on the optical spectra in the oligo-PV and oligo-FL systems and the effect of the dihedral angle on the optical spectra in the amine-FL systems. In the latter study, we take into account the thermal effect by taking the thermal average for the conformations with different dihedral angles between the amine and neighboring FL. Furthermore, we study the electronic structure of amine-fluorene copolymers. Since the localized state may be affected by the edge in short chains, one needs to adopt a fairly long chain to get rid of this unnecessary effect.

As mentioned in the section above, one of our main interests is in the molecular design. Since the photoluminescence spectra in liquid and solid are similar in some of our polymers, we adopt the isolated chain model in which interactions between chains are not taken into account, whereas the crystalline arrangement easily involves the three dimensional effect, which is thoroughly studied [20, 24].

Prior to our TDDFT calculations, all structural optimizations have been carried out using a conventional molecular orbital calculation [18]: the structure optimization of the ground state is carried out at the level of HF/6-31G\*, and that of the excited state is done at the level of CIS/6-31G\*; for the long chains, FL<sub>10</sub>-(amine)-FL<sub>10</sub> and FL<sub>21</sub>, the structure optimizations have been exceptionally performed at the level of AM1 due to the limitation of computational size. The ground state structures are used for the calculations of the absorption spectra, and the excited state structures are used for the calculations of the emission spectra.

PPV and its derivatives have been intensively studied both experimentally and theoretically as their potential applicability to PLEDs [20–23]. The structures of oligo-PV<sub>*n*</sub> in our calculations are shown in figure 1, where *n* represents the number of repeating units. Since it is difficult to study the optical response of the polymer itself, we have modeled oligo-PV<sub>*n*</sub> with different lengths, and estimated the extrapolated values as the polymer properties. The understanding of the relation between the oligomer length and the optical property is essential information to design new molecules,

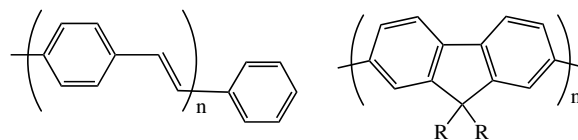


**Figure 1.** Structures of oligo-PV<sub>*n*</sub> (left) and oligo-FL<sub>*n*</sub> (right), where *n* is the number of repeating units.

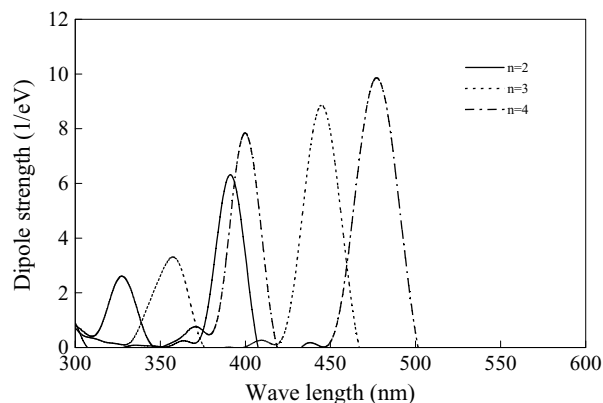


**Figure 2.** Optical properties of oligo-FL dimer ( $n = 2$ , solid line), trimer ( $n = 3$ , dashed line), and tetramer ( $n = 4$ , dot-dashed line).

and thus polymers. We have observed that the peak energy decreases as the number *n* increases. In order to estimate the polymer property, the peak energy is plotted as an inversely proportional function with *n* and extrapolated at  $n = \infty$ . The estimated peak energy is  $\sim 1.93 \text{ eV}$ , which is smaller than the experimentally observed energy of  $\sim 2.2 \text{ eV}$  [22]. This inconsistency is due to the problem of  $V_{xc}$  as mentioned above, which underestimates the band gap.

As a blue emitting material in PLED, FL has been intensively studied [19, 25–27]. The structure of oligo-FL<sub>*n*</sub> is also shown in figure 1. For this material, we have performed the calculations of oligomers with  $n = 2, 3$ , and 4, and the absorption spectra are shown in figure 2. The peak wavelengths are estimated at 391, 444, and 476 nm for  $n = 2, 3$ , and 4, respectively. These values should be compared with the experimentally observed peaks at 329, 350, and 362 nm. This systematic overestimation of peak wavelength is due to the inherent problem in DFT as mentioned above. Keeping this overestimation of peak wavelength in mind, we have compared the absorption and fluorescence spectrum profiles between the TDDFT calculation for  $n = 2$  and the experiment in figure 3. The overall spectrum shapes are quite similar, suggesting the Stokes shift can be well reproduced. One may consider this as an additional advantage of the real-time approach as the spectrum profile in the whole energy range can be obtained in a single calculation.

As practical polymers in PLEDs, fluorene-amine copolymers are frequently used, and the electronic structure around amine is considered to play an important role for the fluorescent spectrum. To study the effect of the dihedral angle on absorption and fluorescence spectra, as shown in figure 4, the spectra of the different conformers in the FL-amine systems have been calculated. All spectra are summed up by the

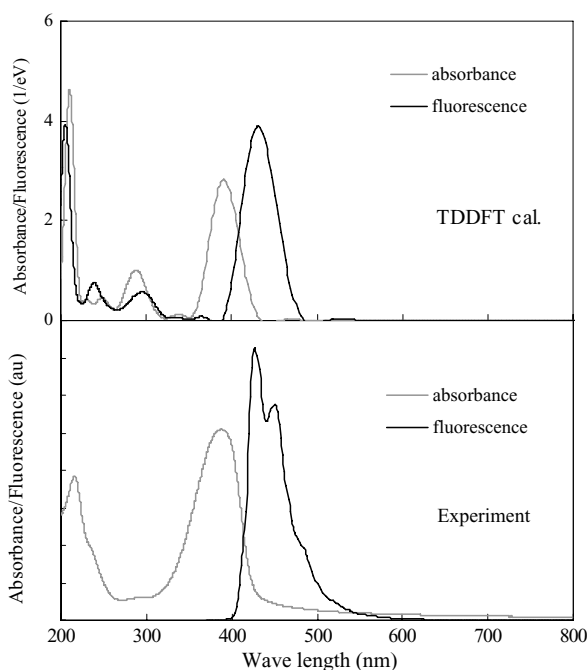


**Figure 3.** Optical properties in the results of TDDFT calculation for oligo-FL and the experiments.

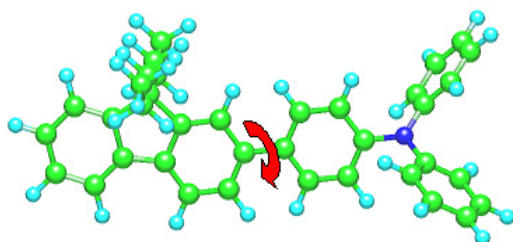


**Figure 4.** Dihedral angle between 9,9-dipropyl-fluorene and triphenylamine.

weighted average for the thermal distribution from the stable structure with the Boltzmann weights at 300 K. The structure is based on the  $S_1$  excited-state potential energy curves of the FL–amine system. The calculation of the  $S_1$  energy has been performed for the dihedral angle  $\theta = 0^\circ$ – $360^\circ$ , with the step of  $\Delta\theta = 30^\circ$ , whereas all the other geometrical parameters are optimized.

Figure 5 shows the emission spectra of FL–FL, FL–triphenylamine (TPA), and FL–phenylenediamine (PDA). In the FL–TPA system, the dihedral angle of  $\sim 0^\circ$  is the most stable in energy, which has the emission spectrum at  $\sim 500$  nm with the highest strength, because the conjugation of the wavefunction is delocalized. When the angle is  $\sim 90^\circ$ , the peak wavelength is blue-shifted; however, the rotational barrier is high enough to minimize the contribution to the spectrum.

The spectra of the other system are also plotted in figure 5. One can see the spectrum dependence on the amine type.

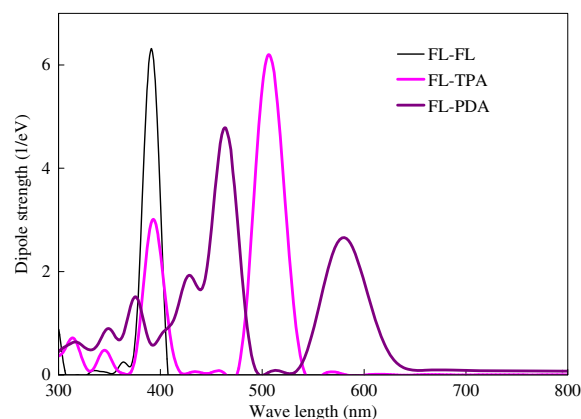


**Figure 5.** Amine dependence of emission spectra.

In particular, the peak wavelength of the FL–PDA system is around  $\sim 600$  nm, longer than the FL–TPA system.

To study the electronic structure of polymers in our model, one needs to consider a fairly long chain to get rid of the edge effect. In a short chain, it may be difficult to recognize the difference between the extended state and the localized state, as some of the latter states may be extended over the short chain. Since we are interested in the difference of the amine types in detail, the electronic structures of FL<sub>10</sub>–(amine)–FL<sub>10</sub> (where amine is TPA or PDA) and FL<sub>21</sub> for the purpose of comparison are calculated. The densities of states (DOSs) of these systems are plotted in figure 6.

We can see a clear band structure of conduction and valence bands for all systems, though the conformations are quite different for each systems. In DOS, there is no significant difference in the electronic structure except for the existence of an additional level in fluorene–amine systems. The additional acceptor level lies just above the valence band and its electronic structure turns out to be localized around the amine. One of the interesting results from DOS is that the TPA-related state is localized in the TPA and the connecting two or three FLs; on the other hand, the PDA-related state is more localized in the PDA and the connecting one or two FLs. The energy level for TPA and PDA systems is  $\sim 0.1$  eV and  $\sim 0.2$  eV from the top of the valence band, respectively. This difference results in longer emission wavelength in FL–PDA than FL–TPA.

#### 4. Conclusions and discussion

TDDFT has been applied to study the optical responses of conjugated polymers. In our calculations, the real-space and real-time approach is used. We have applied the external field to the optimized electronic structure, and followed the time evolution of the dipole moment as a function of time, from which the dynamic polarizability and strength function can be calculated.

Since a real polymer is too large to handle, we have calculated the optical responses of the oligomers, such as oligo-PV and oligo-FL, of different lengths. From the relation between the peak wavelength and the number of repeating units  $n$ , the responses of the polymer are estimated by extrapolation

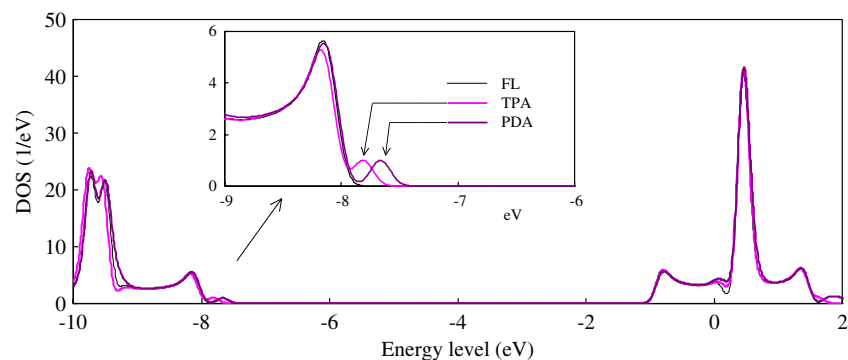


**Figure 6.** Density of states and energy levels of amines.

to  $n = \infty$ . The estimated polymer spectra agree with the experiments reasonably well.

To investigate the effect of the dihedral angle on absorption and fluorescence spectra, we have calculated the spectra of the FL–amine systems, using the thermal distribution weighted average. The spectrum depends on the amine type; in particular, the emission wavelength of FL–PDA is  $\sim 600$  nm, longer than that of FL–TPA.

To study the effects of amine on the electronic structures, DOSs have been studied for the structure of FL<sub>10</sub>–TPA–FL<sub>10</sub>, FL<sub>10</sub>–PDA–FL<sub>10</sub>, and FL<sub>21</sub> for the purpose of comparison. We can see a clear band structure of conduction and valence bands for all systems. In the electronic structure observed from DOS, there is no significant difference in the electronic structure except for the existence of an additional level in fluorene–amine systems. The electronic structure of this additional level turns out to be localized around the amine, and this amine level can be seen as a clear acceptor level in the band gap. The energy level relevant to PDA is deeper at  $\sim 0.2$  eV, whereas that of TPA is a bit shallower at  $\sim 0.1$  eV from the top of the valence band. These are consistent with the results of the FL–amine spectra as mentioned above.

In the application of real-space and real-time TDDFT, the following features are confirmed. In the spectrum calculation, we can obtain fairly good agreement with experimental results through calculations with a relatively small number of grids. To realize this agreement, one has to use long enough time steps in the time evolution as this is related to the accuracy of physical properties of interest. From this point of view, these properties can be conveniently calculated in a required energy region with desired accuracy. We are now confident that TDDFT is a useful computational technique for the material development.

## Acknowledgments

We acknowledge Professor K Yabana for providing his code as our base code and also for useful discussions and encouragements, and N Nishikawa for installing the code to the Earth Simulator, where some of the calculations in this study have been performed.

## References

- [1] Haskal E I, Büchel M, Duineveld P C, Sempel A and van de Weijer P 2002 *MRS Bull.* **27** 864
- [2] Shirakawa H, Louis E J, MacDiarmid A G, Chiang C K and Heeger A J 1977 *J. Chem. Soc. Chem. Commun.* **578**
- [3] Chiang C K, Fincher C R, Park Y W, Heeger A J, Shirakawa H, Louis E J, Gua S C and MacDiarmid A G 1977 *Phys. Rev. Lett.* **39** 1098
- [4] Shirakawa H 2001 *Rev. Mod. Phys.* **73** 713
- [5] Hummer K and Ambrosch-Draxl C 2005 *Phys. Rev. B* **71** 081202(R)
- [6] Brédas J, Cornil J, Beljonne D, Dos Santos D A and Shuai Z 1999 *Acc. Chem. Res.* **32** 267
- [7] e.g. Hummer K, Puschnig P, Sagmeister S and Ambrosch-Draxl C 2006 *Mod. Phys. Lett. B* **20** 261 and the references therein
- [8] Poolmee P, Ehara M, Hannongbua S and Nakatsuji H 2005 *Polymer* **46** 6474
- [9] Runge E and Gross E K U 1984 *Phys. Rev. Lett.* **52** 997
- [10] Dreuw A and Head-Gordon M 2005 *Chem. Rev.* **105** 4009
- [11] Hohenberg P and Kohn W 1964 *Phys. Rev.* **136** B864
- [12] Kohn W and Sham L J 1965 *Phys. Rev.* **140** A1133
- [13] Troullier N and Martins J L 1991 *Phys. Rev. B* **43** 1993
- [14] e.g. Pickett W E 1989 *Comput. Phys. Rep.* **9** 115
- [15] Yabana K and Bertsch G F 1996 *Phys. Rev. B* **54** 4484
- [16] Tateyama Y, Oyama N, Ohno T and Miyamoto Y 2006 *J. Chem. Phys.* **124** 124507
- [17] Chelikowsky J, Troullier N, Wu K and Saad Y 1994 *Phys. Rev.* **50** 11355
- [18] e.g. Kresse G and Purthmüller J 1996 *Phys. Rev. B* **54** 11169
- [19] Frisch M J *et al* 2004 *Gaussian03, Rev. C.02* (Wallingford, CT: Gaussian Inc.) ([http://www.gaussian.com/citation\\_g03.htm](http://www.gaussian.com/citation_g03.htm))
- [20] Yu W L, Cao Y, Pei J, Huang W and Heeger A J 1990 *Appl. Phys. Lett.* **75** 3270
- [21] Ruine A, Caldas M J, Bussi G and Molinari E 2002 *Phys. Rev. Lett.* **88** 206403
- [22] Akino N and Zempo Y 2005 *MRS Proc.* **846** DD.2.3
- [23] Cornil D, Beljonne D, Shuai Z, Hagler T W, Campbell I, Bradley D D C, Brédas J L, Spangler C W and Müllen K 1995 *Chem. Phys. Lett.* **247** 425
- [24] Tian B, Zerbi G, Schenk R and Müllen K 1991 *J. Chem. Phys.* **95** 3181
- [25] Puschnig P and Ambrosch-Draxl C 2005 *Phys. Rev. Lett.* **89** 056405
- [26] Wang J F, Feng J K, Ren A M, Liu X D, Ma Y G, Lu P and Zhang H X 2004 *Macromolecules* **37** 3451
- [27] Brière J F and Côté M 2004 *J. Chem. Phys. B* **108** 3123
- [28] Grice A W, Bradley D D C, Bernius M T, Inbasekaran M, Woo E P and Wu W W 1998 *Appl. Phys. Lett.* **73** 629